IN-SITU DAMAGE MONITORING OF CROSS-PLY LAMINATES USING ACOUSTIC EMISSION

Theodoros Loutas [1], George Sotiriadis [1], Alkis Paipetis [2], Dionysios T. G. Katerelos [1], Vassilis Kostopoulos [1], and Steven L. Ogin [3]

[1] Dept. of Mechanical Engineering and Aeronautics, University of Patras, GR-265 04 Patras, Greece
[2] Dept. of Materials Science and Technology, University of Ioannina, 45110 Ioannina, Greece
[3] School of Engineering (H6), University of Surrey, GU2 7XH Guildford, Surrey, UK
paipetis@cc.uoi.gr

ABSTRACT

"Damage tolerance" is used to describe the attribute of a structure associated with the retention of the required residual strength throughout its service life, while irreversible damage mechanisms are active within the structure itself. "Design for damage tolerance" is based on the identification and quantification of the various damage mechanisms that result in the alteration -mainly deterioration- of the material properties. These may result to different material response to thermomechanical loads. In the present paper, transparent glass-fibre reinforced epoxy laminates were used to study the damage evolution sequence under tensile loading. In parallel, Acoustic Emission (AE) was employed as a non-destructive technique for the in-situ monitoring of the active damage mechanisms until the final failure of the material. Pattern recognition algorithms were utilised to classify and associate the acquired AE signals to the material's damage mechanisms. Experimental findings were compared to theoretical model predictions.

1. INTRODUCTION

The term "damage tolerance" has been used to define the attribute of a structure which enables it to retain its required residual strength for a period of usage and after sustaining specific levels of damage. A prerequisite for damage tolerant design is the identification of the damage mechanisms and their effect on the material response. For multidirectional composite systems, matrix cracking of the off-axis laminates is considered the primary mode of damage as the result of complex combinations of thermal and mechanical loading. This damage mode is also referred to as "transverse" or "intra-laminar" cracking, since the cracks are oriented transversely to the loading direction and is the initial mode of damage to appear first in such composite systems. Transverse cracking has been studied extensively by several researchers over the last 25 years [1-4], focussing mainly on cross-ply glass fibre reinforced polymer composite systems. These material systems are excellent for crack monitoring which is performed via the matching of the refractive index of the fibres and the epoxy resin. In this way, they can be made transparent and thus, the optical observation of the crack development is feasible. The cracks in the off-axis layers usually propagate along the whole width of the specimens parallel to the fibres direction of the corresponding off-axis laminae. The crack density, which is a parameter that characterises these systems and is defined as the number of cracks normalised by the length of the specimen, depends on many parameters. Load level, layer orientation with respect to the load direction, temperature change, number of fatigue cycles, laminate stacking sequence, ply thickness and material fracture toughness are the most important. Damage development in the form of transverse matrix cracking reduces the stress-bearing ability of individual layers resulting in the deterioration of the laminate's thermo-elastic properties.

In order to associate the increase of the crack density versus loading with the resulting thermo-elastic properties reduction, cross-ply composite laminates have been extensively tested under both static and fatigue loading. Experimental techniques used to determine the crack density increase with increasing loading and, subsequently, the resulting thermoelastic properties reduction, involve primarily the testing of composite laminate under both static [1-12] and fatigue [13] loading. Crack density increase is measured by

optical microscopy, while the stiffness reduction in the form of longitudinal Young's modulus and Poisson's ratio is determined from the recorded stress-strain curves. Laser Raman spectroscopy [14-18] has proved to be a highly accurate method for the measurement of crack density as a function of applied strain when combined with the determination of macroscopic quantities such as the residual strain due to cracking and the longitudinal Young's modulus reduction.

Significant research effect has been put in the study of the matrix cracking development and the resulting properties degradation covering a broad range from micromechanics to continuum damage mechanics [1-4]. The theoretical analyses relate to experimental measurements and vary in sophistication: shear-lag analyses, more rigorous elasticity analysis, variational mechanics and finite elements solutions are all available in the literature. In general, these analyses differ in the determination of the approximate local stress distributions between two cracks in a representative volume element. The derived stress state is then applied to determine the corresponding thermo-elastic constants. More rigorous solutions which involve complex numerical routines are presented in [19-20]. More complex laminate system than the simplest cross-ply configuration were analyzed by using the suggested "equivalent constraint model" (ECM) [21-23] in order to calculate the effective properties of the damaged layer. For these lay-ups, finite element analysis in conjunction with experimental data has also been employed [24-26]. The crack face relative displacements are reported to govern the stiffness reduction [27-28]. The suggestion presented is to neglect the effect of neighbouring layers on crack face displacements and to use the known solution for a periodic system of cracks in an infinite homogeneous transversely isotropic medium (90-layer). Since in this approach the constraint layer is replaced by 90-layer, the calculated values are independent on the relative ply stiffness ratios. For example, according to FEM calculations performed in [28] the crack opening displacement (COD) is indeed insensitive to the constraint layer and cracked layer stiffness ratio for composites with high anisotropy. However, the numerical COD values calculated using approach in [27-28] are overestimated by 20% for internal cracks and by 30% for external cracks. For glass fibre composites the anisotropy is lower and the constraint layer can be with less error replaced by the 90-layer material. The approach by Lundmark and Varna [29-31] presents the stiffness and thermal expansion coefficients of an arbitrary symmetric laminate with cracks in certain layers in an exact and explicit form and accounts also for crack interaction.

In the present paper glass fibre reinforced cross-ply composite specimen are loaded in tension to study and identify the damage mechanisms that are active until the specimen failure. Acoustic Emission (AE) activity was recorded during the tests and utilising unsupervised pattern recognition algorithms the damage modes were identified and their evolution in time was revealed. The crack density increase with increasing applied strain is calculated using the energy based approach [32]. The optical identification and correlation of the transverse cracking to the acoustic activity of the specific damage mechanism enabled the identification of two additional damage mechanisms which continued to be active until the failure of the specimens.

2. EXPERIMENTAL

2.1 Materials fabrication

Cross-ply laminates were fabricated by employing a modified frame-winding technique, which is described in details in previous works [6, 14, 17]. Typical E-glass fibres were winded around a rectangular steel first in one direction, which would be the 90° lamina and following in the transverse direction to form the 0° lamina. A Shell "Epicote" 828 epoxy resin was used cured with nadic methyl-anhydride and accelerator K61B in the ratio 100:60:4 mixed and degassed before impregnation. The composite system was cured between thick glass plates under 100 kg of weight for 3h at 100 °C, followed by a

post cure at 150 °C for another 3h. The fibres volume fraction of the laminates fabricated was 0.63%. A 2.52-mm laminate was thus manufactured with a 90° ply thickness of 0.62-mm and a 0° ply thickness of 0.64-mm. By matching the refractive indices of the epoxy matrix and the E-glass fibres the manufactured composites are transparent, which allows the in-situ optical observation and recording of the macroscopic damage (in the form of intra- and inter-laminar cracking) development. Tensile specimens were cut from the laminates following the ASTM D3039 standard.

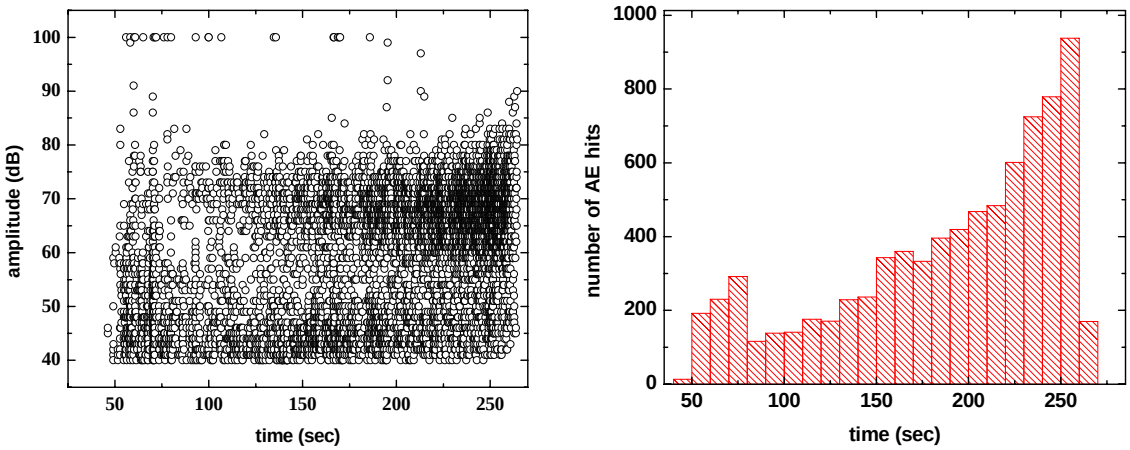

(a) (b)

Figure 1: Acoustic Emission activity during a typical tensile test. (a) Amplitude of the AE activity and (b) distribution of AE hits over time.

2.2 Tensile Testing

All tensile tests were performed using an Instron Universal Testing Machine equipped with hydraulic gripping system, under displacement control, at controlled environmental conditions of 25 °C and 70% relative humidity. AE activity was recorded during the tensile testing of the materials (Fig. 1a & b).

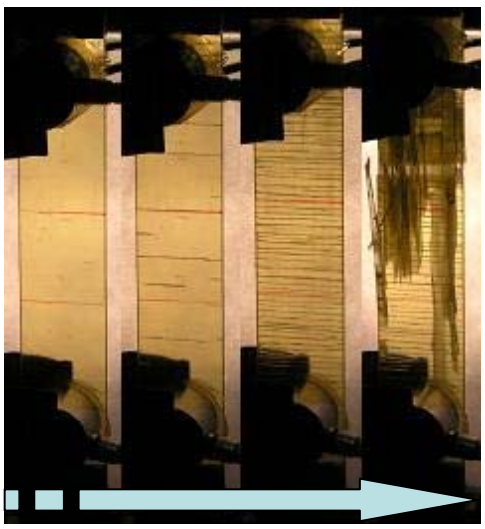

Figure 2: The crack accumulation in the gauge length of the cross ply specimens. The red lines denote the gauge length for the derivation of strain data. On the top and the bottom of the specimen the AE sensors can be seen

2.3 Acoustic Emission Monitoring

Acoustic emission activity was continuously monitored during the quasi-static tensile

tests of the specimens. The acquisition parameters for the two active channels were: threshold and gain equal to 40 and 20 dB, respectively, while the peak definition time (PDT), hit definition time (HDT) and hit lockout time (HLT), were set at 50, 100 and 500 μs respectively. The data acquisition system used was a PCI-2 data acquisition board from Physical Acoustics Corporation. The AE signals were monitored by using two pico broadband transducers, which were attached to each specimen by means of a suitable coupling agent (molybdenum grease). Pre-amplification of 40 dB and band pass filtering of 20-1200 kHz was performed on the recorded AE signals by 2/4/6-AST pre-amplifiers. Pencil break tests were conducted for the calibration of the set up and the fine tuning of the Δt front-end filters which prevented the acquisition of AE hits outside a predefined gauge length. Fig. 1 summarizes the AE activity during a typical test.

3. RESULTS

3.1 Tensile Testing – Strain Measurements

Tensile tests were conducted according to ASTM D3039 standard method. The transverse cracking accumulation was monitored with concurrent photographing of the cracking process with a frequency of 30 s^{-1} and the strain was derived from the photographs from the relative displacement of horizontal lines positioned on the sample (Fig. 2). A typical stress & number of cracks vs. time curve is shown in Fig. 3.

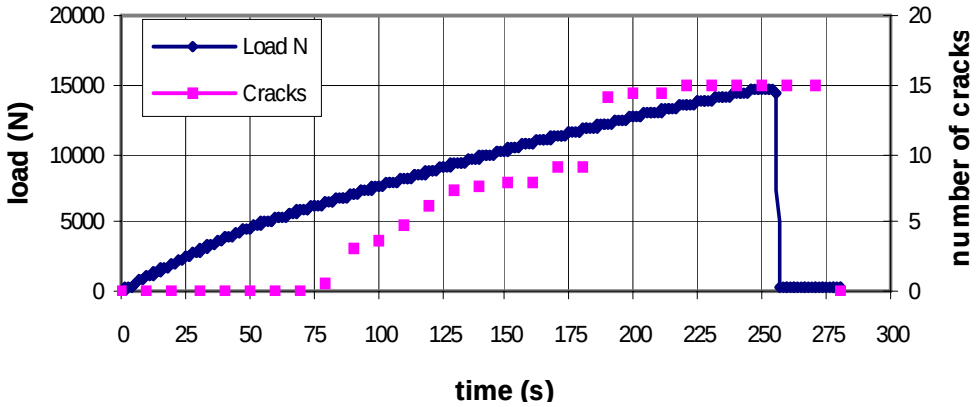

Figure 3: Load and number of cracks measured in the gauge length fo a typical tensile experiment.

3.2 Acoustic Emission and Unsupervised Pattern Recognition

Unsupervised pattern recognition algorithms were utilized in order to classify the recorded AE waveforms and identify the material's dominant damage mechanisms. The procedure followed is described elsewhere analytically [33-34]. A combination of *Maxmin distance* and *Isodata* algorithms produced the final clustering resulting in 3 classes. These classes are completely separated in the 4^{th} dimensional space (four is the dimension of the pattern vectors formed) and the separation can even be seen in a 2-D projection (Fig. 4). The pattern recognition scheme applied for the specific clustering was based on pattern vectors composed of the following five descriptors: amplitude, rise angle, initiation frequency and mechanical load. Cluster validity criteria such as R and τ criteria [35-36] were applied to confirm the successful separation of the AE population.

4. DISCUSSION

4.1 Stress dependent damage accumulation and optical damage identification

The load vs. time dependence is shown in Fig. 3. At approximately 50 sec a characteristic knee appeared in the curve, denoting the end of the linear elastic region and the initiation of irreversible damage. Although the softening of the material was obvious, transverse cracks along the entire width of the specimen did not appear before 75 sec after the onset

of the experiment. The transverse cracking continued to accumulate smoothly until approximately 175 sec and increased rapidly near the saturation value thereafter. However, complete saturation within the monitoring length was reached at 220 sec. The final failure of the sample followed shortly afterwards at approximately 250 sec.
As was expected, the typical load time curve was characterised by two distinct areas which are separated by the onset of degradation caused by the matrix cracking. The saturation on the other hand is not as obvious, as other damage mechanisms are by then active which interact with the shear discontinuities caused by the transverse cracks.

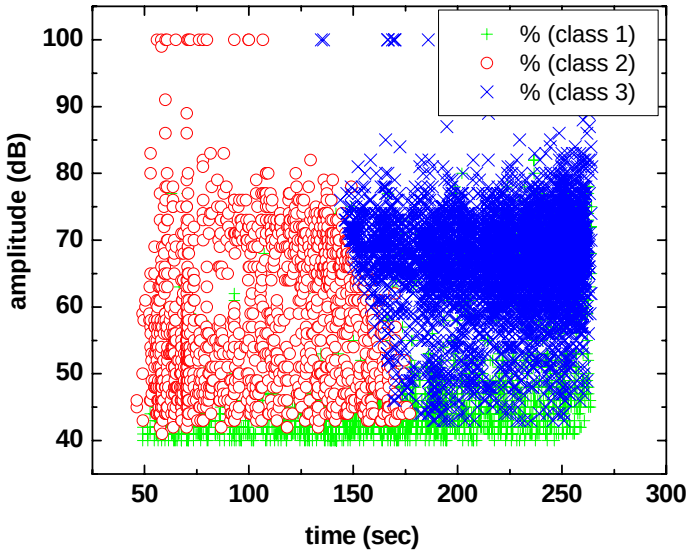

Figure 4: Separation of resulted classes in 2-D projection.

4.2 Modelling of the transverse cracking induced degradation

The degradation caused via the matrix cracking is the most studied area in the load time (or strain) response of the cross ply laminate. This degradation is clearly defined by the appearance of the transverse cracks and is completed when saturation is reached.
An energy based criterion has been proposed recently by Katerelos et al [32] for the determination of damage evolution in cross-ply composites. This criterion is based on the determination of the Strain Energy Release Rate, G_c, using the energy that is dissipated during the loading of a cross-ply composite laminate. Alternatively, the G_c is calculated from the relationship between the stiffness reduction and the applied strain. Combining these two ways, a theoretical relationship between the crack density (number of cracks per unit length) and the applied strain can be extracted. A necessary step in this procedure is to choose an appropriate analytical model for the determination of the stiffness degradation as a function of applied strain. In the case presented here the stiffness reduction model used is the one proposed by Lundmark and Varna [29].
The critical Strain Energy Release Rate for the formation of cracks has been calculated from the tensile data, which were extracted from the stress-strain curve. Knowing, at a specific strain level the number of cracks formed (N) and the corresponding Young's Modulus (E_x), together with the specimen geometrical characteristics (length L = 250 mm, width w = 25 mm, thickness h = 2.5 mm and 90° ply thickness h_{90} = 1.22 mm) the G_c is calculated by the following relationship (1)

$$G_c = \frac{1}{2}\varepsilon^2 L \frac{h}{h_{90}} \frac{E_x}{N} \qquad (1)$$

The strain (ε) level used was 0.4% where 3 cracks are formed and the corresponding E_x is 18.2 GPa. Thus the critical Strain Energy Release Rate calculated was G_c = 49.7 kJ/m^2.
Then, the following equation is used to extract the relationship between the crack density

(ρ) and the applied strain

$$G_c = \frac{1}{2}\varepsilon^2 \frac{h}{h_{90}} \frac{E_0}{\left(1 + A_0\, \rho\, u_0\right)^2} A_0 u_0 \tag{2}$$

E_0 is the initial Young's Modulus (E_0 = 27 GPa). A_0 is a constant introduced by Lundmark and Varna [31] and is given by

$$A_0 = \frac{E_T}{E_0} \frac{2\, h_{90}}{h_{90} + 2\, h_0} h_{90} \tag{3}$$

where E_T is the transverse Young's Modulus (E_T = 14.27) and h_0 is the 0° ply thickness (h_0 = 1.22 mm). According to the studies performed by Lundmark and Varna [31] the crack opening displacement (u_0) in an internal layer can be represented by the following power law

$$u_0 = A_m + B_m \left(\frac{E_T}{E_L}\right)^{n_m} \tag{4}$$

where the constants A_m, B_m and n_m are given by following empirical forms

$$\begin{aligned} A_m &= 0.52 \\ B_m &= 0.3075 + 0.1652 \left(\frac{h_{90} - 2\, h_0}{2\, h_0}\right) \\ n_m &= 0.030667 \left(\frac{h_{90}}{2\, h_0}\right)^2 - 0.0626 \left(\frac{h_{90}}{2\, h_0}\right) + 0.7037 \end{aligned} \tag{5}$$

Damage in the form of cracking at increasing tensile loading levels as calculated using the described model is presented in Fig. 5. The theoretical predictions are plotted against experimental data that were extracted from the photographs sequence taken during the experiment.

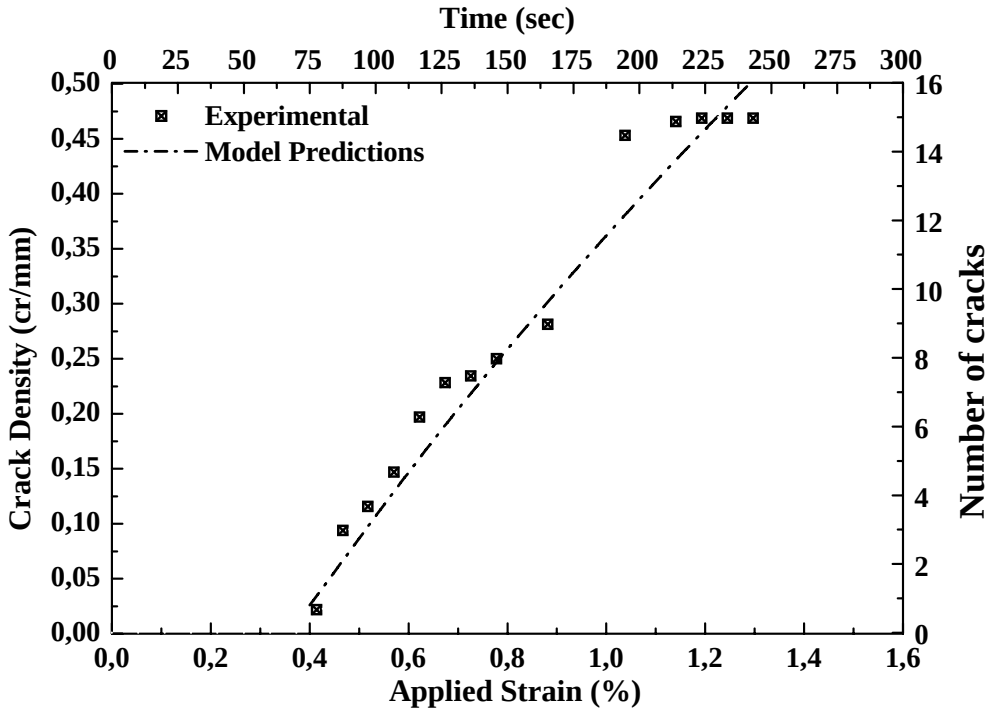

Figure 5: Prediction of the Crack density as a function of applied strain.

Experimental data in Fig. 5 showed that crack density increased until it reached a point where no additional cracks were formed. This point, which in the case studied here was

at about 1.1% applied strain, is called “cracking saturation point”. Model predictions fitted well the experimental data. The saturation point is not accurately predicted although the applied strain value that corresponds to this crack density value was very close to the experimental values. This can be attributed to the fact that the model is based on and describes very well only one damage mechanism that is, transverse cracking. As is explained elsewhere herein, several damage mechanisms are present during the loading history of the specimen, such as interfacial failure, fibres fracture and matrix yielding. Consequently, whereas until the saturation point matrix cracking is the dominant damage mechanism from that point onward the other mechanisms and especially fibres breakage dominate up to the specimen’s final fracture. The other mechanisms involve among others delamination, fibre breakage and debonding, matrix cracking and yielding. Whereas analytical models can predict the degradation due to matrix cracking, a failure criterion must be employed in order to predict the saturation stage.
In this study, the evaluation of the Acoustic emission that follows, allows for the identification and the partial quantification of the other damage mechanisms that essentially envelop the transverse cracking and cumulatively lead to the failure of the cross ply composite coupon.

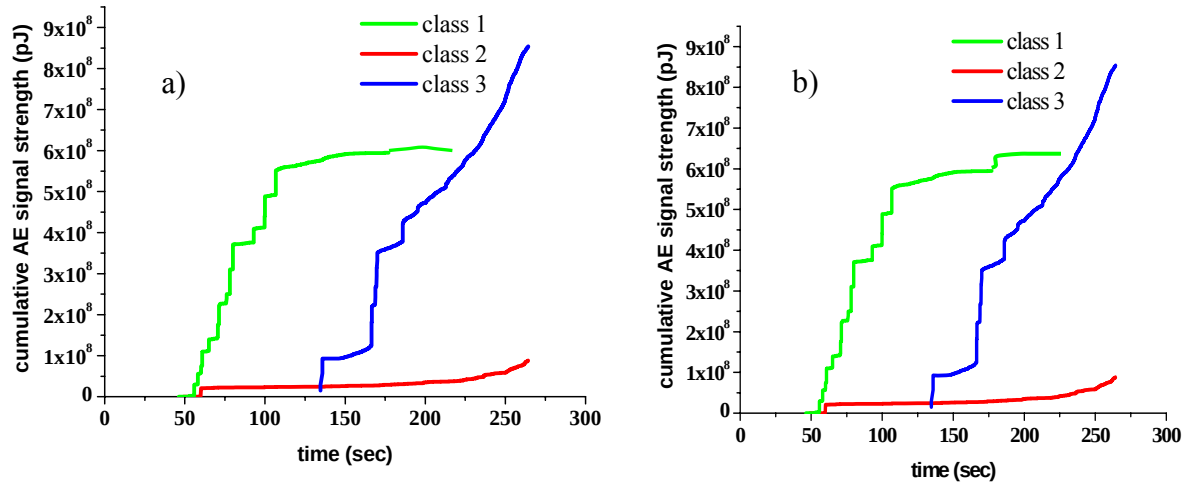

Figure 6: a) Cumulative number of AE hits versus test time b) Cumulative AE signal strength versus test time

4.4 AE signals Classification

In order to correlate the resulted classes of AE data with the material’s damage mechanisms two types of graphs are particularly useful. The cumulative number of AE hits versus time (Fig. 6a) and the cumulative AE signal strength versus time (Fig. 6b). Fig. 6a reveals the initiation and evolution of each class during the test time.
The acoustic activity was divided in three distinct classes. The most important observation at this stage was that the first two classes coincide with the notable “knee” in the load time curve which, as postulated previously, corresponds to the onset of irreversible damage. Class 1 was the first class activated just a few seconds earlier than class 2. As class 1 contained significantly higher energy content (Fig. 6b) it was attributed to matrix cracking. Class 1 became active prior to the appearance of complete transverse cracks and became silent after saturation was reached that is at approximately 225 seconds. It is therefore clearly attributed to the 90 ply cracking. The early onset of the class 1 activity can be attributed to (i) cracks outside the monitored length, (ii) incomplete cracks and (iii) the time that a transverse crack needs to bridge the edges of the specimen.
Class 2 is active throughout the whole period that AE is emitted from the test specimen. Its energy content (signal strength) is quite lower than class 1 and 3. It is attributed to

fibre/matrix interface phenomena such as interfacial sliding and interfacial bond failure. These secondary damage mechanisms are active at the locus of any discontinuity. Class 2 precedes class 1, as the minor defects accumulate in order to trigger major damage mechanisms, such as matrix cracking in the beginnings, or cumulative fibre failure of the longitudinal plies which lead to the fracture of the specimen.
Finally, class 3 dominated in terms of both AE hits and AE signal strength. It started to be active at about 140 sec and remains highly active until the end of the test. It is attributed to single and multiple fibre failures that dominate the final stages of the material's life, and lead to the final failure of the composite. The late onset is due to the stress limit that must be reached in order for fibre failures to be statistically significant.

5. CONCLUSIONS

Transparent glass fibre reinforced cross ply composites were tested in tension in order to identify the damage mechanisms involved in their failure. Load, time and optical monitoring of the crack accumulation were used in conjunction with the recording of the acoustic activity of the specimens. The characteristic areas of the load time curve were identified and confirmed with optical observations. The acoustic emission signals were classified using unsupervised algorithms and the derived clusters were identified in conjunction with the load time curves as well as the optical observations. The crack accumulation was successfully modelled using an energy based criterion. This damage mode together with two more principal damage mechanisms were identified using the acoustic emission imprint derived from the unsupervised clustering. These damage modes were the primary modes associated to transverse cracking and fibre failure as well as a secondary mode active throughout the time span when irreversible damage is taking place and is attributed to minor deterioration at the loci of shear discontinuities which accumulate to trigger major damage.

ACKNOWLEDGEMENTS

This work has been funded by the European Community and Greek National funds through the Operational Program for Educational and Vocational Training (EPEAEK II), "PYTHAGORAS II".

REFERENCES

1. Talreja, R. *"Damage characterization by internal variables"*. In: Pipes, R.B. and Talreja, R., editors. *Damage mechanics of composite materials*. Composite materials series, vol. 9. Amsterdam: Elsevier; 1994.
2. Nairn, J. and Hu, S. *"Matrix microcracking"*. In: Pipes R.B., Talreja R, editors. *Damage mechanics of composite materials*. Composite materials series, vol. 9. Amsterdam: Elsevier; 1994.
3. Varna, J., Joffe, R., Akshantala, N.V. and Talreja, R. "Damage in composite laminates with off-axis plies", *Composites Science & Technology*, 1999; 59(14): 2139-2147.
4. Nairn, J. *"Matrix microcracking in composites"*. In: Kelly, A., Zweben, C., Talreja, R. and Manson, J. – A., editors. *Polymer matrix composites.* Comprehensive composite materials, vol. 2. Amsterdam: Elsevier; 2000.
5. Boniface, L., Ogin, S. L. and Smith, P.A. "Fracture mechanics approaches to transverse ply cracking in composite laminates". *ASTM STP*, 1991; 1110: 9-29.
6. Crocker, L. E., Ogin, S. L., Smith, P. A. and Hill, P. S. "Intra-laminar fracture in angle-ply laminates", *Composites Part A*, 1997; 28(9-10): 839-846.
7. Smith, P. A. and Ogin, S. L. "On transverse matrix cracking in cross-ply laminates loaded in simple bending", *Composites Part A*, 1999; 30: 1003-1008.
8. Smith P. A. and Ogin, S. L. "Characterization and modelling of matrix cracking in a

$(0/90)_{2s}$ GFRP laminate loaded in flexure", *Proceedings of the Royal Society of London A*, 2000; 456 2755-2770.
9. Joffe, R. and Varna, J. "Analytical modeling of stiffness reduction in symmetric and balanced laminates due to cracks in 90° layers", *Composites Science & Technology*, 1999; 59(11): 1641.
10. Varna, J., Joffe, R. and Talreja, R. "A synergistic damage-mechanics analysis of transverse cracking in $[\pm\theta/90_4]_s$ laminates", *Composites Science & Technology*, 2001; 61, 657-665.
11. Varna, J., Joffe, R. and Talreja, R. "Mixed micromechanics and continuum damage mechanics approach to transverse cracking in $[S, 90_n]_s$ laminates", *Mechanics of Composite Materials*, 2001; 37(2): 115-126.
12. Rubenis, O., Spārniņš, E., Andersons, J. and Joffe, R. "The Effect of Crack Spacing Distribution on Stiffness Reduction of Cross-Ply Laminates", *Applied Composite Materials*, 2007; 14(1): 59-66.
13. Tong, J., Guild, F. J., Ogin, S. L. and Smith, P.A. "Off-axis fatigue crack growth and the associated energy release rate in composite laminates", *Applied Composite Materials*, 1997; 4: 349-359.
14. Katerelos, D. G., Galiotis C., Ogin, S. L. and Whattingham, R. D. "Determination of stiffness reduction and residual strain caused by transverse cracking using an embedded aramid fiber strain sensor", In: Composites from fundamentals to exploitation. *Proceedings of ECCM9*, Brighton, UK; 2000 [Proc. in CD-ROM].
15. Parthenios, J., Katerelos, D. G., Psarras, G. C. and Galiotis, C. "Aramid fibres: a multifunctional sensor for monitoring stress/strain fields and damage development in composite materials", *Engineering Fracture Mechanics*, 2002; 69(9): 1067-1078.
16. Katerelos, D. G. and Galiotis, C. "Axial strain redistribution resulting from off-axis ply cracking in polymer composites", *Applied Physics Letters*, 2004; 85(17): 3752-3754.
17. Katerelos, D. G., McCartney, L. N. and Galiotis, C. "Local strain re-distribution and stiffness degradation in cross-ply polymer composites under tension", *Acta Materialia*, 2005; 53(12): 3335-3343.
18. Katerelos, D. T. G., Lundmark, P., Varna, J. and Galiotis, C. "Analysis of matrix cracking in GFRP laminates using Raman spectroscopy", *Composites Science & Technology*, 2007; 67(9): 1946-1954.
19. Schoeppner, G. A. and Pagano, N. "Stress fields and energy release rates in cross-ply laminates", *International Journal of Solids and Structures*, 1998; 35(11): 1025-1055.
20. McCartney, L. N., Schoeppner, G. A. and Becker, W. "Comparison of models for transverse ply cracks in composite laminates", *Composites Science & Technology*, 2000; 60(12-13): 2347-2359.
21. Zhang, J., Fan, J. and Soutis, C. "Analysis of multiple matrix cracking in $[\pm\theta_m/90_n]_s$ composite laminates. Part 1. In-plane stiffness properties", *Composites*, 1992; 23(5): 291-304.
22. Kashtalyan, M. and Soutis, C. "Stiffness degradation in cross-ply laminates damaged by transverse cracking and splitting", *Composites Part A*, 2000; 31(4): 335-351.
23. Katerelos, D. T. G., Kashtalyan, M., Soutis, C. and Galiotis, C. "Matrix Cracking in Polymeric Composite Laminates: Modelling and Experiments", *Composites Science & Technology*, 2007; doi:10.1016/j.compscitech.2007.09.013.
24. Tong, J., Guild, F. J., Ogin, S. L. and Smith, P.A. "On matrix crack growth in quasi-isotropic laminates. Part II. Finite element analysis", *Composites Science & Technology*, 1997; 57(11): 1537-1545.
25. Marsden, W. M., Guild, F. J., Ogin, S. L. and Smith, P.A. "Modelling stiffness-damage behaviour of $(\pm45/90)_s$ and $(90/\pm45)_s$ glass fibre reinforced polymer laminates", *Plastics Rubber and Composites*, 1999; 28(1): 30-39.

26. Pradhan, B., Venu Kumar, N. and Rao, N. S. “Stiffness degradation resulting from 90° ply cracking in angle-ply composite laminates”, *Composites Science & Technology*, 1999; 59(10): 1543-1552.
27. Gudmundson, P. and Östlund, S. “First order analysis of stiffness reduction due to matrix cracking”, *Journal of Composite Materials*, 1992; 26(7): 1009-1030.
28. Gudmundson, P. and Zang, W. “A universal model for thermoelastic properties of macro-cracked composite laminates”, *International Journal of Solids and Structures*, 1993; 30(23): 3211-3231.
29. Lundmark, P. and Varna, J. “Constitutive relationships for damaged laminate in in-plane loading”, *International Journal of Damage Mechanics*, 2005; 14(3): 235-259.
30. Lundmark, P. and Varna, J. “Crack face sliding effect on stiffness of laminates with ply cracks”, *Composites Science & Technology*, 2006; 66(10): 1444-1454.
31. Lundmark P. and Varna, J. “Stiffness reduction in laminates at high crack density: effect of crack interaction”, *International Journal of Damage Mechanics*, 2005 [submitted for publication].
32. Katerelos, D. T. G., Varna, J. and Galiotis, C. “Energy criterion for modelling damage evolution in composites”, *Composites Science & Technology*, 2007; doi:10.1016/j.compscitech.2007.09.014.
33. V. Kostopoulos, T. H. Loutas, A. Kontsos, G. Sotiriadis and Y. Z. Pappas, On the identification of the failure mechanisms in oxide/oxide composites using acoustic emission, NDT & E International, Volume 36, Issue 8, December 2003, 571.
34. V. Kostopoulos, T. Loutas and K. Dassios, Fracture behavior and damage mechanisms identification of SiC/glass ceramic composites using AE monitoring, Composites Science and Technology, Volume 67, Issues 7-8, June 2007, Pages 1740-1746
35. Fukunaga K., Introduction to statistical pattern recognition, 2nd English ed. San Antonio, CA, USA: Academic Press; 1990.
36. Tou JT, Gonzales RC., Pattern recognition principles. Reading, MA:Addison-Wesley; 1974.